LA-UR -78-913

CONF-780806-1

TITLE: NUMERICAL MODELING OF THE DEFLAGRATION-TO-DETONATION TRANSITION

AUTHOR(S): Charles L. Mader

SUBMITTED TO: 17th International Symposium on Combustion
Leeds, England
August 20-25, 1978

los alamos
scientific laboratory
of the University of California
LOS ALAMOS, NEW MEXICO 87545

An Affirmative Action/Equal Opportunity Employer

DISTRIBUTION OF THIS DOCUMENT IS UNLIMITED

Form No. 836
St. No. 2629
1/78

UNITED STATES
ENERGY RESEARCH AND
DEVELOPMENT ADMINISTRATION
CONTRACT W-7405-ENG. 36

MASTER

NUMERICAL MODELING OF THE DEFLAGRATION-TO-DETONATION TRANSITION

CHARLES A. FOREST AND CHARLES L. MADER

Los Alamos Scientific Laboratory
University of California
Los Alamos, New Mexico

The effect of a confined porous bed of burning explosive in contact with a solid explosive is studied by computer simulation. The burning is modeled using a bulk burn model that is a function of the surface area and the pressure. Once pressure excursions occur from the confined burning the transition to detonation is modeled using a pressure-dependent heterogeneous explosive shock decomposition model called Forest Fire. The occurrence of detonation in the solid explosive is shown to be dependent upon the surface-to-volume ratio, the confinement of the porous bed, and the geometry of the system.

Introduction

In some circumstances a burning high explosive or high-energy propellant will detonate. The change from burning to detonation is known as the Deflagration-to-Detonation Transition (DDT). Accidents with high explosives and propellants often involve DDT.

A linear burn of an explosive proceeds at a rate of 10 to 100 cm/s, whereas a detonation wave propagates at a rate of 0.3 to 0.9 cm/μs. The rates are very different and special conditions are necessary for the transition from burning to detonation to occur. Conditions conducive to the occurrence of DDT are the confinement of a burning region with a large surface area and a nearby material of high shock sensitivity. The surface area may be initially present or may be dynamically produced as a result of stress on the material. The confinement is provided both by the material strength and the inertia of the confining material. The presence of a large burning surface area increases the mass burn rate over that of the linear rate and can result in high pressures and the formation of shocks. If the shock is strong enough, the explosive begins to decompose, the shock grows, and finally a detonation is produced.

The burning in a porous bed is known as convective combustion. In addition to the role of high mass burning rate and confinement, the flow of hot gas relative to the bed of particles is often important, especially in a large porous bed. The flowing gases enter into the fluid dynamics (a two-phase flow problem) and transfer

heat to the particles. Ignition, flame spreading, and flame structure in the voids may also be involved. Burning of gun propellants involves many of these processes.

Rather than try to model such a collection of processes, a model is constructed which involves only confined burning and shock initiation. The cases considered involve mostly solid explosive, a small region of porous material, and adequate confinement. Such situations may relate better to accidents since it seems unlikely that a piece of explosive will turn entirely to dust because it is dropped. A small region of porous material may be too small to produce a DDT by itself. However, if the small region is in contact with a large piece of solid explosive, there is the possibility that detonation may occur in the solid. The burning of the porous material need not proceed at detonation rates but needs only burn fast enough to form a shock in the adjacent solid. If the solid is sensitive to shock-induced decomposition and the shock is strong enough, the shock will grow into a detonation wave.

The shock initiation of detonation of a heterogeneous explosive has been recently numerically modeled using the Forest Fire method[1] for describing the rate of decomposition of an explosive as a function of the local shock pressure. The model has been used to describe the propagation and failure of heterogeneous detonation waves along surfaces and around corners.[2]

The decomposition that occurs by shock interactions with density discontinuities is described by a burn rate determined from

the experimentally measured distance of run to detonation as a function of shock pressure (the Pop plot), the reactive and non-reactive Hugoniot, and the assumption that the reaction rate derived near the front can be applied throughout the flow.

With Forest Fire to describe the transition once pressure excursions occur from the confined burning, numerical modeling of the process of burning to detonation requires a model for burning.

The bulk burn model is used to simulate the burning of a porous bed of explosive or propellant that is assumed to be ignited over all burning surfaces simultaneously. The explosive is assumed to be divided into uniform pieces of similar geometry which burn at the linear burn rate perpendicular to the surface of each particle. The change in burning surface area as the particles are consumed is included. The model for surface area change is motivated by three special geometric situations; namely (1) sphere-like particles, volumes which contain an inscribed sphere, (2) cylinder-like particles, volumes which contain an inscribed cylinder, and (3) sheet-like particles, volumes which have constant surface area. In the first two cases the surface area and volume of the particles are functions of the radius of the inscribed sphere or cylinder only. In each case there exists a q so that (surface area/initial surface area) = (volume/initial volume)^{q} with q = 2/3 for sphere-like, q = 1/2 for cylinder-like, and q = 0 for sheet-like particles. However, q may assume any value to simulate mixtures of particle types.

Bulk burn is a simplified treatment of the process known as convective combustion. In convective combustion hot gases from the burn flow into the porous bed ahead of the burning region. The flowing hot gases heat the cold particles until ignition and enter into the fluid dynamic features (two-phase flow). In spite of the simplifications, bulk burn is appropriate for small confined regions where gas motion during ignition and during burning is small.

The Bulk Burn Model

The usual burn under confinement proceeds on the surface of the explosive with a rate that increases with pressure to some power. It is important to describe the surface area available for burning and the pressure-dependent rate law of burning. This is called the bulk burn model.

The model for bulk burning was constructed using the following assumptions.

a. The mass of propellant burns on a surface area S such that the burn proceeds normal to the surface according to the linear burn rate $\frac{dX}{dt}$ (for example $\frac{dX}{dt} = cP^n$).

b. For the purposes of the burning model only, the density of the burning explosive is constant.

The bulk burning model may be described by

$$\frac{dW}{dt} = - (S/V)_o W^q \frac{dX}{dt} \quad ,$$

where

$(S/V)_o$ = initial burn surface-to-volume ratio,

$\frac{dX}{dt}$ = linear burn rate,

q = geometry dependent exponent with $0 \leq q \leq 1$,

W = mass fraction of unburned explosive.

Some specific cases for q:

$q = 0$, constant surface area burn

$q = 1/2$, cylinder-like particles burn

$q = 2/3$, sphere-like particles burn.

Assuming each particle burns at a rate $\frac{dX}{dt}$ perpendicular to its surface, the time derivative of mass, M, is

$$dM/dt = -S\rho \frac{dX}{dt} \quad ,$$

$$dM/dt = -(S_o/V_o)(S/S_o)(\rho_o V_o)(\rho/\rho_o) \frac{dX}{dt} \quad .$$

Let $(S/S_o) = (M/M_o)^q(\rho/\rho_o)^{-q} = (\rho V/\rho_o V_o)^q(\rho/\rho_o)^{-q}$;

then

$$dW/dt = -(S_o/V_o)(\rho/\rho_o)^{1-q} W^q \frac{dX}{dt} \quad ,$$

where

V_o = initial volume,

M = mass of solid explosive,

ρ = density of solid explosive,

S = surface area burning,

S_o = initial surface area.

The motivation for

$$(S/S_o) = (M/M_o)^q(\rho/\rho_o)^{-q}$$

comes from the consideration of three special cases for plane-, cylinder- and sphere-like polyhedral particles.

For plane-like particles we have

$$S = S_o \quad , \; Vol = S\ell$$
$$(S/S_o) = 1 = (Vol/Vol_o)^o \quad ,$$

where ℓ is the thickness of particles.

For cylinder-like particles (containing an inscribed cylinder and ignoring the surface area of the ends) we have

$$S = Ar\ell \quad , \quad Vol = Ar^2\ell/2$$
$$(S/S_o) = (r/r_o) = (Vol/Vol_o)^{1/2} \quad ,$$

where r is the radius of the cylinder and ℓ is length of the cylinder.

For sphere-like particles (containing an inscribed sphere) we have

$$S = Ar^2 \quad , \quad Vol = Ar^3/3$$
$$(S/S_o) = (r/r_o)^2 = (Vol/Vol_o)^{2/3} \quad ,$$

where r is the radius of the sphere.

In the above cases A is a constant depending on the shape of the particles, 2π for cylinders, 4π for spheres, 24 for cubes, and 8 for square tubes.

In each of the above cases

$$(S/S_o) = (Vol/Vol_o)^q \quad , \text{ for some } q.$$

Thus

$$(S/S_o) = (\rho\ Vol/\rho_o\ Vol_o)^q(\rho/\rho_o)^{-q}$$

and

$$(S/S_o) = (M/M_o)^q(\rho/\rho_o)^{-q} = W^q(\rho/\rho_o)^{-q} \quad .$$

Since $(\rho/\rho_o)^{-q}$ is approximately one we have

$$\frac{dW}{dt} = -(S/V)_o W^q \frac{dX}{dt} \quad .$$

Calculations

The SIN[3] one-dimensional Lagrangian hydrodynamic code was used to perform the calculations. The Forest Fire rate for the low density (ρ = 1.72) explosive was calculated from the high density (ρ = 1.91) explosive experimental Pop plot and Forest Fire rate by a technique assuming invariance with density of the shock wave particle velocity as a function of time to detonation and single curve build-up as described in reference 4.

To obtain a full hydrodynamic simulation of burning to detonation, the problem considered was the burning of a segment of low density explosive adjacent to high density explosive. A sequence of problems varying the confinement, the burn rate, and the geometry was calculated using explosive parameters and burn parameter approximating HMX of $q = 2/3$, $\frac{dX}{dt}$ (cm/μsec) = $0.007728\ P^{0.942}$, and $(S/V)_o$ of 75/cm and 100/cm corresponding to spheres of 0.4- and 0.3-mm radius.

The four problem geometries are shown in Fig. 1. Two types of confinement are considered. In one type the porous region is between solid explosive and an aluminum case which can move into air (problem geometries I and II). In the second type the porous region is contained in solid explosive alone (problem geometry III). Three geometries are included--planar (problem geometry I), cylindrical converging (problem goemetry II), and cylindrical diverging (problem geometry III). The mass burn in the porous region is simulated using the bulk burn model. Bulk burn assumes that the porous region is composed of particles of similar geometry with some initial surface-to-volume ratio (S_o/V_o). For each problem geometry, calculations are made for various (S_o/V_o). The bulk burn rates for (S_o/V_o) = 75 and 100 are displayed in Fig. 2.

Shock-induced decomposition of the solid explosive is simulated with the Forest Fire model. In these problems the decomposition rate is taken to be a function of pressure only. Also displayed in Fig. 2 are the Forest Fire rates at densities $\rho = 1.91$ and $\rho = 1.72$ as a function of pressure. The initial calculational cell length in each region is 0.1 cm.

To illustrate the effect of a low-density (high shock sensitivity) region contained within the solid explosive, one problem is shown using problem geometry IV. In this case a 1.0-cm slab of $\rho = 1.72$ explosive is embedded in the solid and reacts using the Forest Fire model.

The results of the calculations are shown in Figs. 3-7. In each frame of the figures is shown a graph of pressure as a function of distance and a graph of mass fraction as a function of distance. The pressure scale is given in the lower right corner (e.g. 50 kbar); the mass fraction scale is always 0 to 1.0. Time is indicated on each frame in microseconds. The initial surface-to-volume ratio $(S/V)_o$ for the bulk burn region is as specified for each figure.

Comparison of the problems gives some insight into the importance of the various boundary conditions, geometric symmetry, and processes. The 1-D plane geometry problems (I) show the effect of varying the surface-to-volume $(S/V)_o$ ratio. The $(S/V)_o$ of 100 results in detonation as shown in Fig. 3 and fails to cause detonation if $(S/V)_o$ is 75 as shown in Fig. 4.

The cylindrical converging geometry problem (II) results in detonation with an $(S/V)_o$ of 75 as shown in Fig. 5. The cylindrical diverging geometry problem (III) fails to cause detonation with an $(S/V)_o$ of 100 as shown in Fig. 6. This illustrates the balance between the bulk burn and the diverging wave which lowers the pressure. The case of $(S/V)_o = 130$ detonates just prior to the wave reaching the outer case, whereas $(S/V)_o = 100$ fails to detonate. Comparison of these to the planar and cylindrical converging problems shows that geometry is a very significant factor in the ultimate outcome.

Problem geometry IV is similar to problem geometry I except for the inclusion of a 1.0-cm region of lower density explosive. The problem with $(S/V)_o$ = 75 shows detonation occurs about 1.4 cm into the ρ = 1.91 explosive past the lower density region as shown in Fig. 7. The presence of the low density region noticeably alters the pressure wave even though detonation did not occur in the 1.72 g/cc explosive region. The pressure wave as incident on the 1.72 g/cc explosive region is too low to cause detonation to occur in a 1.0-cm run; however it is sufficient to induce significant partial decomposition which adds to the wave causing detonation in the adjacent high density explosive.

Conclusions

This study has examined some of the conditions leading to detonation in a solid explosive bounded by a confined porous burning region. Items important to occurrence of detonation are (1) the surface area burning, (2) the confinement of the burning region, (3) the geometry of the system, and (4) the shock sensitivity of the adjacent solid material. Items (1), (2), and (3) work together to produce the pressure waves which generate shocks in the solid. Geometry is especially critical in this regard; a system which may not produce detonation in planar geometry may well induce detonation in converging geometry. The solid material shock sensitivity determines the response to the shocks generated. The planar geometries (I and IV) with $(S/V)_o$ = 75 illustrate this

effect well. Only a portion of the solid explosive adjacent to the burning region need be more sensitive to go from a nondetonating condition to a detonating one.

This study suggests that realistic numerical modeling of the burning to detonation process is possible. Further development of the model should permit numerical simulation of experimental observations of burning to detonation and result in increased understanding of this challenging problem.

Acknowledgments

We gratefully acknowledge the contributions of Bobby G. Craig, Jerry D. Wackerle, and Louis C. Smith of the Los Alamos Scientific Laboratory. This work was partially supported by the Department of the Navy, Strategic Systems Project Office.

REFERENCES

1. MADER, C. L. and FOREST, C.A.: Two-Dimensional Homogeneous and Heterogeneous Detonation Wave Propagation, Los Alamos Scientific Laboratory Report LA-6259, 1976.
2. MADER, C. L.: Two-Dimensional Homogeneous and Heterogeneous Detonation Wave Propagation, Sixth Symposium (International) on Detonation, ACR-221, p. 405, 1976.
3. MADER, C. L. and GAGE, W. R.: FORTRAN SIN--A One-Dimensional Hydrodynamic Code for Problems Which Include Chemical Reactions, Elastic-Plastic Flow, Spalling, and Phase Transitions, Los Alamos Scientific Laboratory Report LA-3720, 1967.
4. FOREST, C. A.: Burning and Detonation, Los Alamos Scientific Laboratory, unpublished data, 1978.

FIGURE CAPTIONS

1. Problem geometries for explosive burning to detonation calculations.
2. Forest Fire shock decomposition rates for explosive at two densities and bulk burn rate for explosive at $\rho = 1.72$ and $(S/V)_o = 75$ and 100/cm.
3. SIN calculation for the 1-D plane problem geometry I with $(S/V)_o = 100/cm$.
4. SIN calculation for the 1-D plane problem geometry I with $(S/V)_o = 75/cm$.
5. SIN calculations for the 1-D cylinder problem geometry II with $(S/V)_o = 75/cm$.
6. SIN calculation for the 1-D cylinder problem geometry III with $(S/V)_o = 100/cm$.
7. SIN calculation for the 1-D plane problem geometry IV with $(S/V)_o = 75/cm$.

1-D PLANE

Problem Geometry I (Figs. 3 and 4)

AIR 2 cm	ALUMINUM 2 cm	HE (1.91) 10 cm FOREST FIRE	HE (1.72) 2 cm BULK BURN	ALUMINUM 2 cm	AIR 2 cm

1-D CYLINDER

Problem Geometry II (Fig. 5)

CENTER •	HE (1.91) 10 cm FOREST FIRE	HE (1.72) 2 cm BULK BURN	ALUMINUM 2 cm	AIR 2 cm

Problem Geometry III (Fig. 6)

CENTER •	HE (1.72) 2 cm BULK BURN	HE (1.91) 10 cm FOREST FIRE	ALUMINUM 2 cm	AIR 2 cm

1-D PLANE

Problem Geometry IV (Fig. 7)

AIR 2 cm	ALUMINUM 2 cm	HE (1.91) 5.5 cm FOREST FIRE	HE (1.72) 1.0 cm FOREST FIRE	HE (1.91) 3.5 cm FOREST FIRE	HE (1.72) 2 cm BULK BURN	ALUMINUM 2 cm	AIR 2 cm

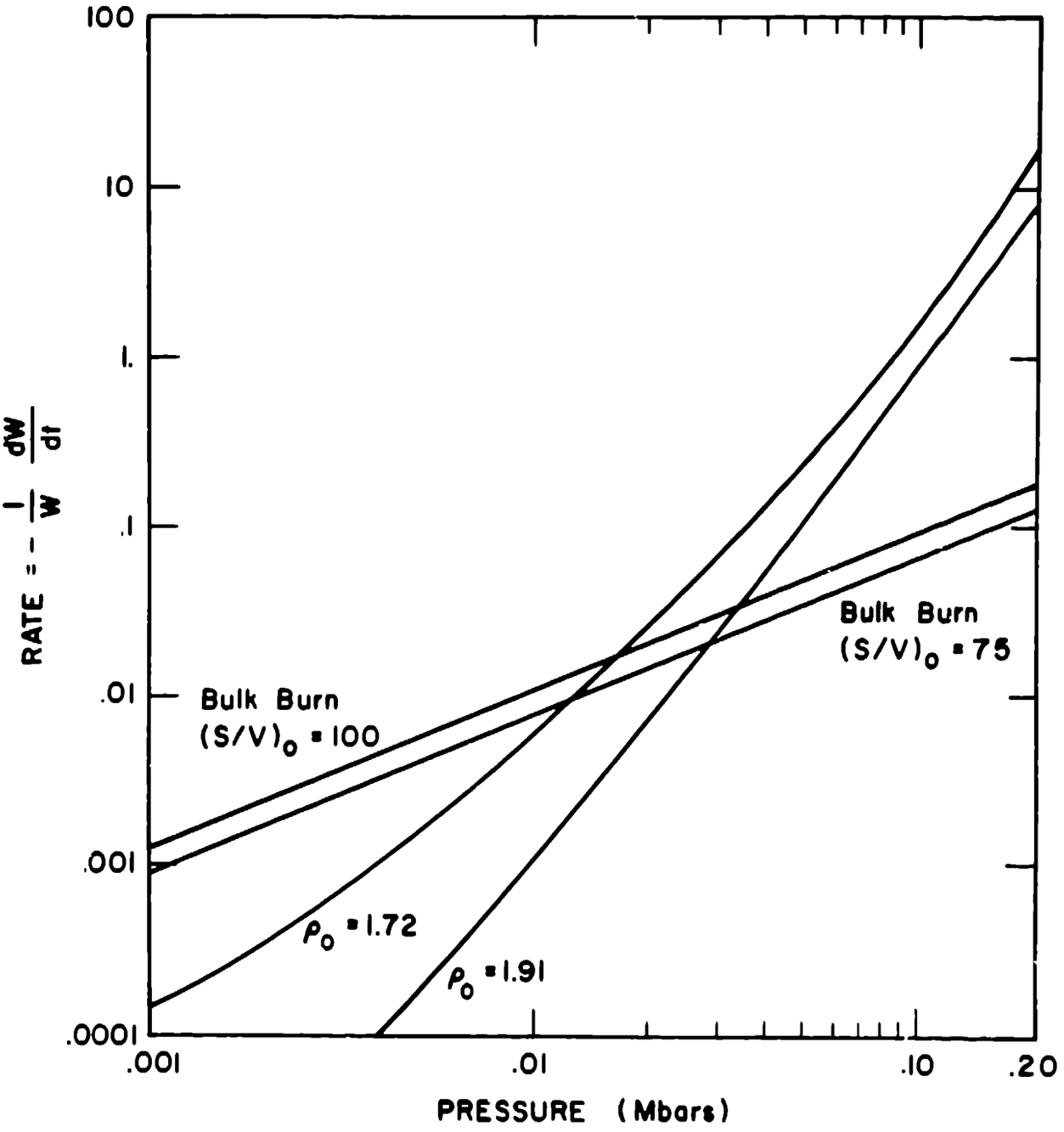
100
10
1.
.1
.01
.001
.0001
RATE = - 1/W dW/dt
Bulk Burn
(S/V)0 = 100
Bulk Burn
(S/V)0 = 75
ρ0 = 1.72
ρ0 = 1.91
.001
.01
.10
.20
PRESSURE (Mbars)

Fig 3

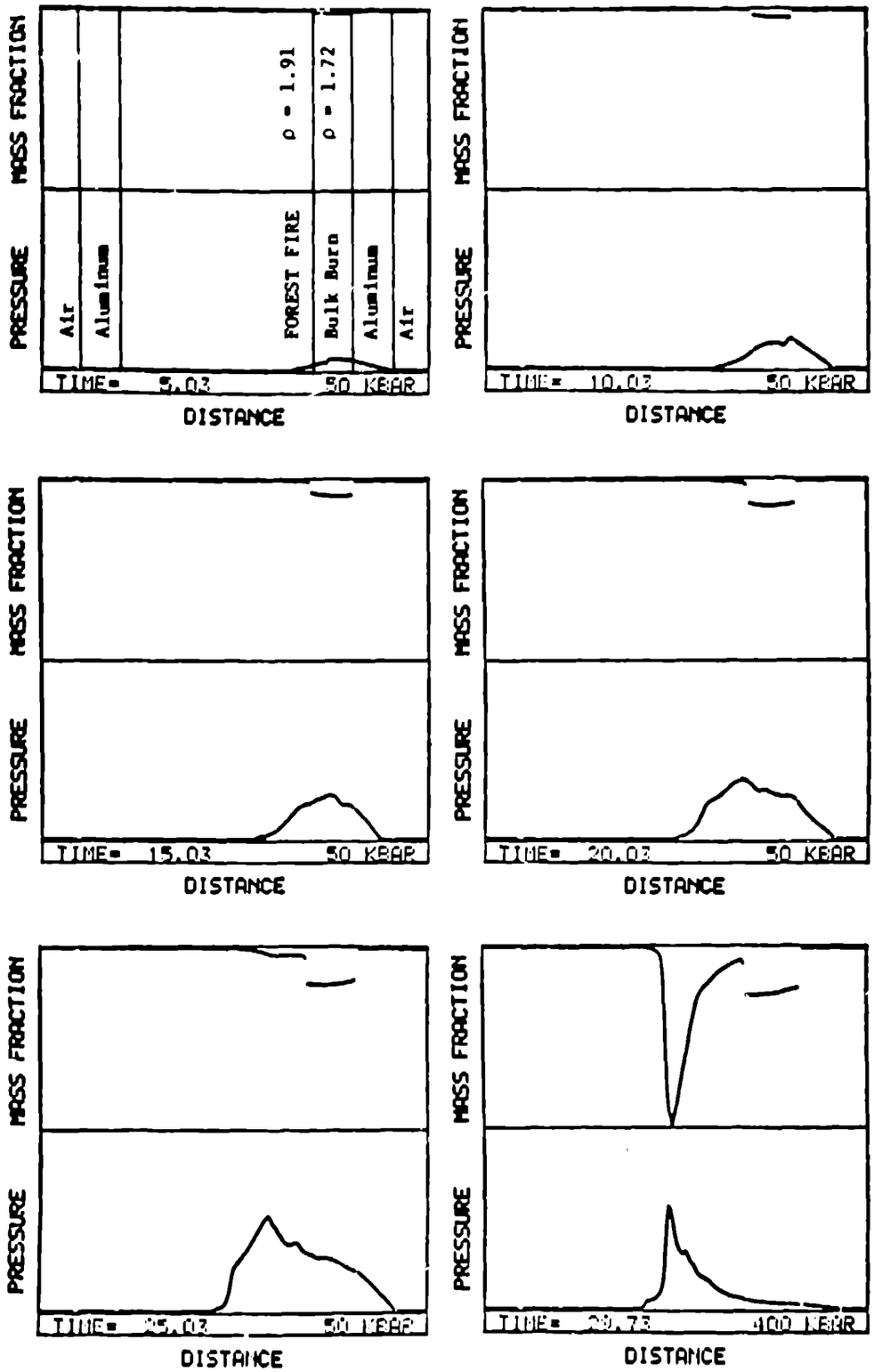

1-D PLANE

$(S/V)_0$ = 100/cm

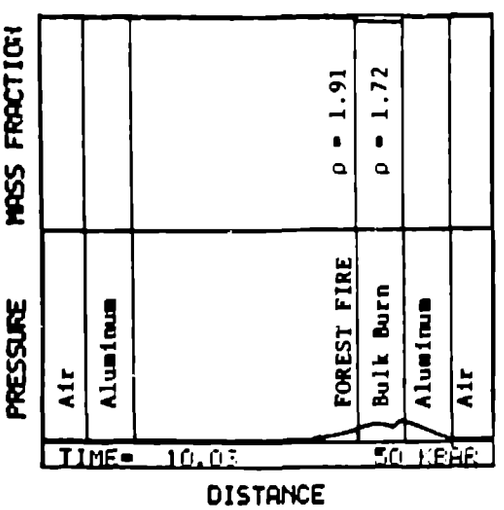

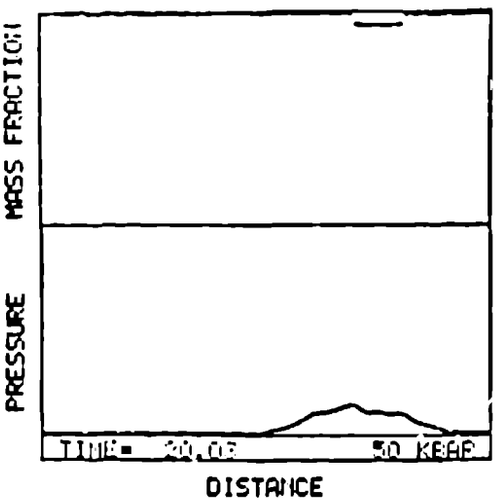

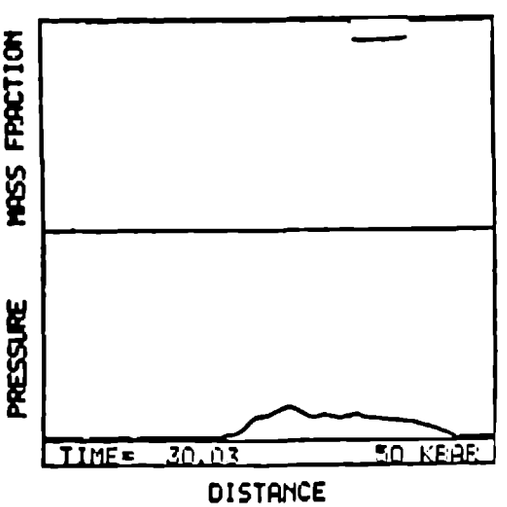

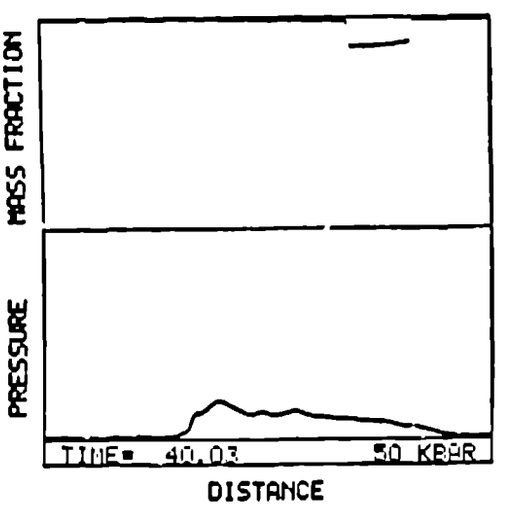

1-D PLANE

$(S/V)_0$ = 75/cm

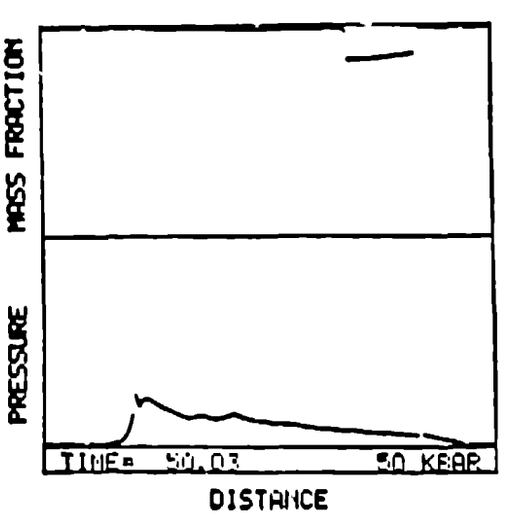

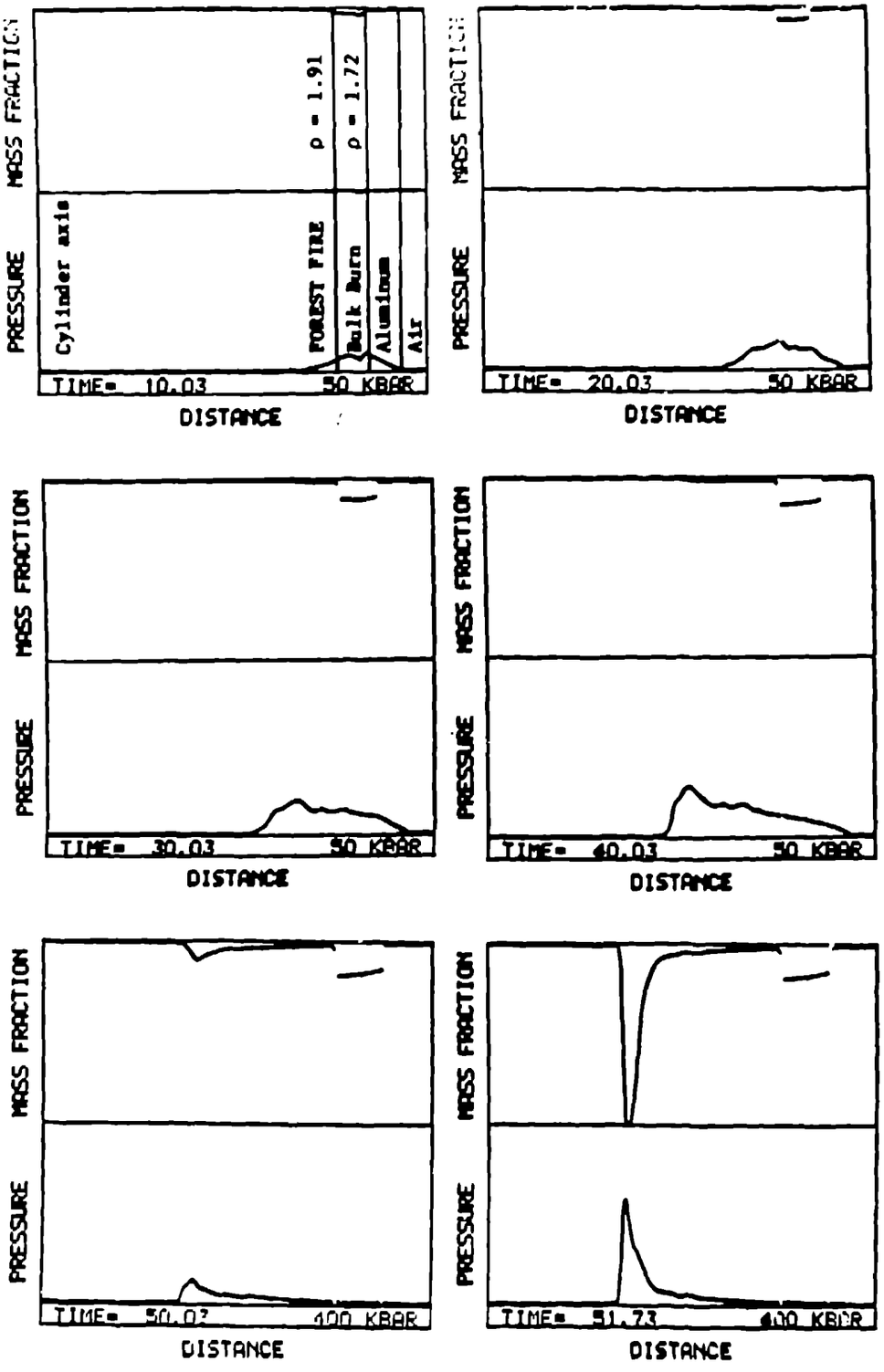

1-D CYLINDER $(S/V)_0 = 75/cm$

PROBLEM GEOMETRY (II)

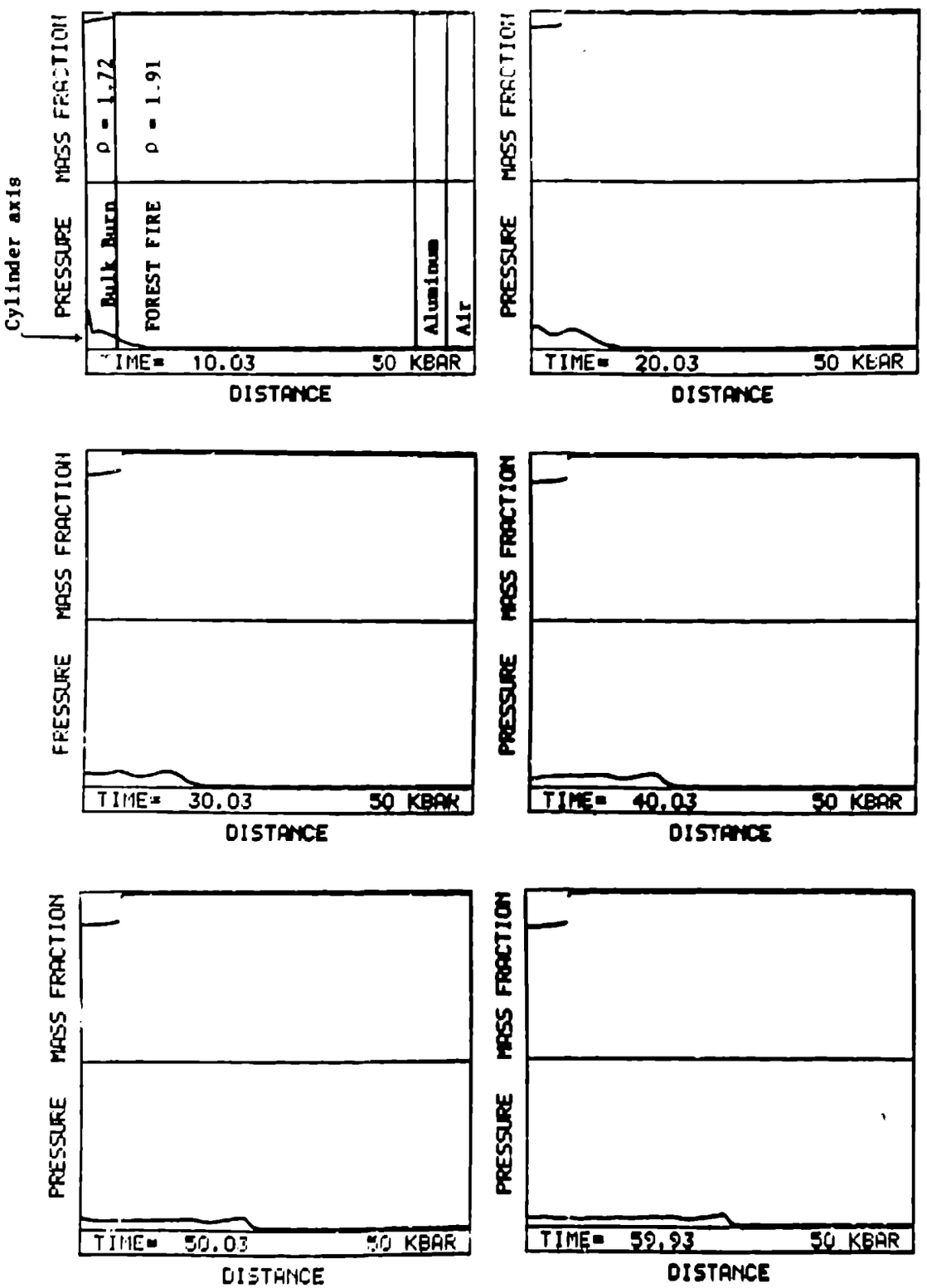

1-D CYLINDER $(S/V)_0 = 100/cm$

PROBLEM GEOMETRY (III)

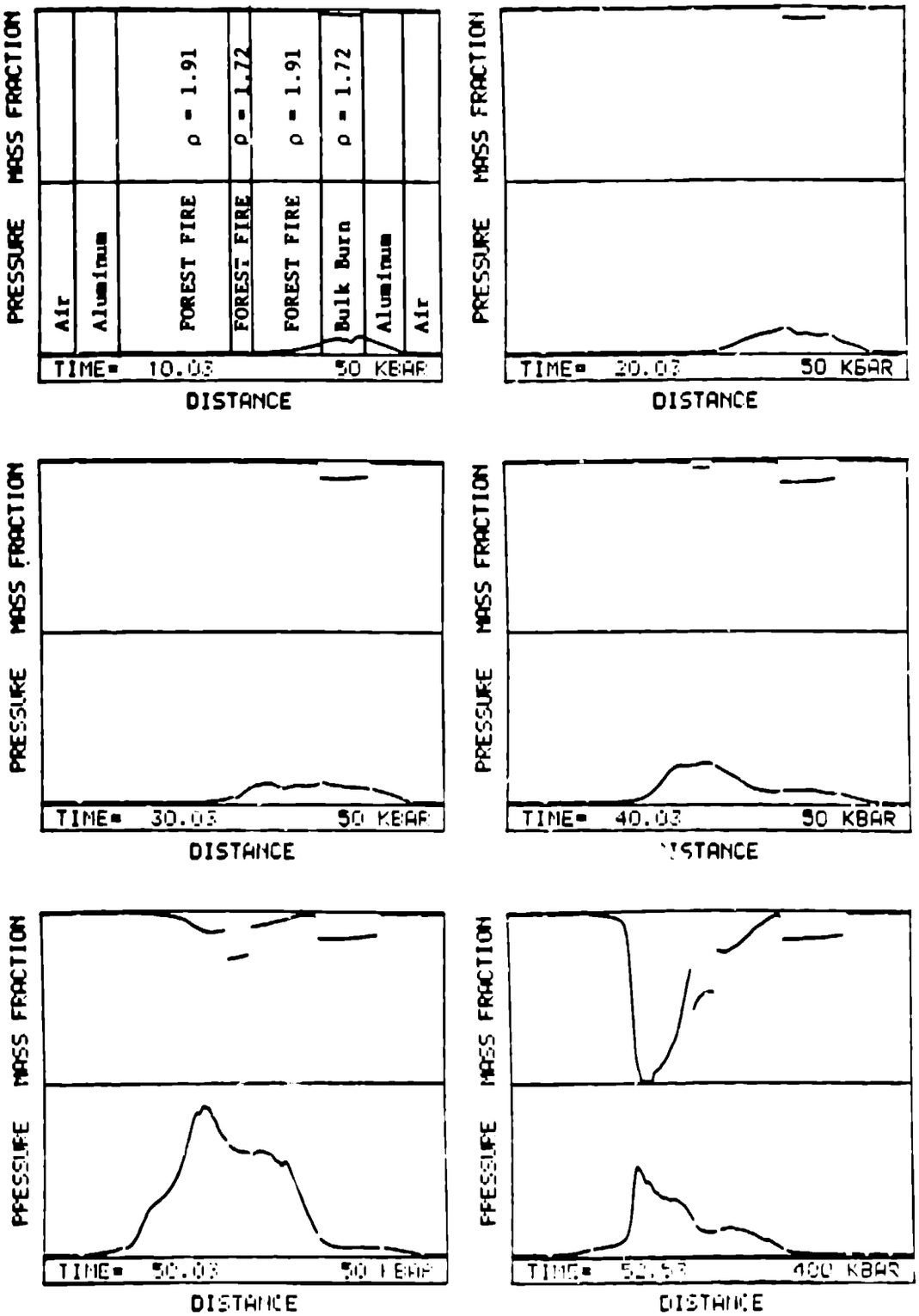

1-D PLANE

PROBLEM GEOMETRY (IV)

$(S/V)_0$ = 75/cm